Nuclear Instruments and Methods in Physics Research B 268 (2010) 3315–3320

Contents lists available at ScienceDirect

Nuclear Instruments and Methods in Physics Research B

journal homepage: www.elsevier.com/locate/nimb

Comparison of candidate secondary electron emission materials

Z. Insepov [a,*], V. Ivanov [b], H. Frisch [c]

[a] Mathematics and Computer Science Division, Argonne National Laboratory, Argonne, IL, USA
[b] Muons Inc., Batavia, IL, USA
[c] High-Energy Physics Division, Argonne National Laboratory, Argonne, IL, USA

ARTICLE INFO

Article history:
Received 23 April 2010
Received in revised form 21 June 2010
Available online 8 August 2010

Keywords:
Secondary electron emission
Micro-channel plate
Materials
Monte Carlo method

ABSTRACT

Secondary electron emission (SEE) yields obtained with empirical models deviate significantly from experiment. Therefore they cannot be used to predict the SEE data for various materials. The angular dependencies of SEE in empirical models are also drastically different and inconvenient for comparison. SEE coefficients were calculated by a theoretical method that uses Monte Carlo simulation, empirical theories, and close comparison to experiment, in order to parameterize the SEE yields of highly emissive materials. We have successfully applied this method to bulk Al_2O_3, a highly emissive material for micro-channel plates, as well as to thinly deposited films of Al_2O_3. The simulation results will be used in the selection of an emissive material, and if the emission yield of the material is small, as a resistive material for the deposition and characterization experiments that will be conducted by a large-area fast detector project at Argonne National Laboratory.

1. Introduction

Theoretical studies of secondary electron emission (SEE) yields are important for developing computational tools capable of calculating the SEE yields for a range of high-SEE-yield engineering materials (emissive materials) that can be used in particle detectors for high-energy physics, such as Cherenkov, neutrino, and astroparticle detectors [1,2]. Secondary electrons also play a significant role in visualizing micron-sized patterns in scanning electron microscopy (SEM); theory and simulation of SEE are therefore a large part of SEM development [3,4,7–15]. Secondary electron emission of surfaces exposed to high-gradient electromagnetic fields is one of the factors of the multipacting effect that can significantly degrade the performance of particle accelerators. Therefore, reducing the SEE yield is a key issue for the development of future accelerators [16]. Fusion devices are also susceptible to SEE, which can cause surface breakdown at high electric gradients [17].

The goal of this work is to develop a parameterized set of the SEE-yield dependencies on two variables, the primary electron energy (E_{PE}) and the angle of incident electrons (θ), for materials of interests in the large-area fast detector development project at Argonne National Laboratory. This parameterization can be done by using results obtained from Monte Carlo calculations with existing codes [3,4,7–9] modified to meet the needs of micro-channel plate (MCP) developments, as well as by using the results of empirical SEE-yield models [18–21]. Modification of the Monte Carlo codes will be necessary to address and include in the database new, highly emissive materials such as MgO and Al_2O_3, and a mixture of ZnO and alumina, which is resistive; such materials are important for new MCP development [5]. The glass MCPs cannot provide the time resolution and spatial resolution that are necessary for large-area photo-detectors [6]. Therefore, the new MCP concept is based on pores fabricated in alumina by means of tools well developed in the semiconductor industry. Since alumina is an insulator, we will also need to study resistive materials that will be used for resistive coating of the MCP pores. The method will be verified with experimental data obtained in the literature and with new data measured specifically for the large-area fast detector project. The calculated yields will also be used as input files for macroscopic MCP gain and transient time calculation codes for computing electron trajectories inside MCPs of various types, such as chevron and funnel. Feedback from the gain code will then be used to improve the materials data and will stimulate further search for the best MCP emissive and resistive materials.

2. Secondary electron emission yields

Secondary electron emission is an important tool for surface microanalysis in various research, science, and industrial areas. Primary electron collisions with the surface of a target generate emissions of various types of secondary electrons [12]:

- "True" secondary electrons having kinetic energies <50 eV (depending on the material, the most probable energy of SEE is about 1–3 eV, and the average energy is between 4 and 5 eV [12]).
- Auger electrons.

* Corresponding author. Tel.: +1 630 252 5049; fax: +1 630 252 5986.
E-mail address: insepov@anl.gov (Z. Insepov).

0168-583X/$ - see front matter © 2010 Elsevier B.V. All rights reserved.
doi:10.1016/j.nimb.2010.08.002

- Elastically reflected backscattered (BS) electrons, having energies 50 eV < E < E_{PE}, where E_{PE} is the primary electron energy.

The following coefficients are defined according to these processes: SE1 is the number of secondary electrons emitted by primary electrons within the escape range, and SE2 is the number of secondary electrons emitted by the backscattered ones on their way back to the surface. SE2 = $\beta\eta *$ SE1, where η is the backscattered yield and β is the efficiency with which backscattered electrons generate the secondary electrons. The total number of secondary electron emissions per primary electron, δ, is the number of electrons emitted with higher energies. The total yield is SE1$(1 + \beta\eta)$ [9].

2.1. Energy dependence

Several researchers have developed semi-empirical theories regarding electron yield [7–13]. Such theories are helpful in calibrating Monte Carlo simulations, which are the main tool for obtaining the SEE yield for various materials at different energies and incident angles of primary electrons.

The SEW yield can be written in the following form [12]:

$$\delta = \int n(x, E_{PE}) f(x) dx, \tag{1}$$

where $n(x, E_{PE})$ is the number of secondary electrons produced at a distance x from the surface by a primary electron with the energy of E_{PE} and $f(x)$ is the probability that the secondary electrons will escape from the surface.

It is assumed that n is proportional to the average energy loss in the target:

$$n(x, E_{PE}) = -\frac{1}{\varepsilon}\frac{dE}{dx}, \tag{2}$$

where ε is the energy per secondary electron emitted at a distance x from the surface. The probability of the secondary electron traveling to the surface and escaping from the surface is as follows:

$$f(x) = Be^{-x/\lambda}, \quad B < 1, \tag{3}$$

where λ is the mean electron escape depth [9,11].

Young [13] showed that the electron energy loss inside the target is approximately constant:

$$-\frac{dE}{dx} = E_{PE}/R, \tag{4}$$

Here R is the electron ranges.

By using the above formulas, we can get a combined SEE yield as follows:

$$\delta = \int_0^\infty \frac{B}{\varepsilon}\frac{E_{PE}}{R} e^{-x/\lambda} dx, \tag{5}$$

$$\delta(E_{PE}) = B\frac{E_{PE}}{\varepsilon}\frac{\lambda}{R}(1 - e^{-R/\lambda}). \tag{6}$$

The electron ranges R in Al_2O_3 were measured by Young [13], who proposed a formula that was in close agreement with Bethe's theory prediction at low electron energies [12]:

$$R/[\mathrm{mg/cm^2}] = 0.0115\left(\frac{E_{PE}}{[\mathrm{keV}]}\right)^{1.35}. \tag{7}$$

If δ_m and E^m are the yield and energy at maximum, respectively, the reduced yield δ/δ_m is independent of the materials constants B, ε, and ρ. This is called a universal curve:

$$\frac{\delta}{\delta_m} = 1.11\left(\frac{E_{PE}}{E^m_{PE}}\right)^{-0.35}\left(1 - e^{-2.3\left(\frac{E_{PE}}{E^m_{PE}}\right)^{1.35}}\right), \tag{8}$$

where E and E^m are the primary electron energies at maximum.

Lin and Joy [8] calculated the ion ranges by a slightly different formula:

$$R = \frac{B}{\rho}(E_{PE})^{1.67}.$$

Here B = 76 nm, E_{PE} is in keV, and ρ is in g/cm^3, giving a different final expression:

$$\frac{\delta}{\delta_m} = 1.28\left(\frac{E_{PE}}{E^m_{PE}}\right)^{-0.67}\left(1 - e^{-1.614\left(\frac{E_{PE}}{E^m_{PE}}\right)^{1.67}}\right). \tag{9}$$

Formulas (8) and (9) are usually referred to as the "universal law of SEE yield" [7–12]. They provide a valuable calibration tool for developing Monte Carlo codes for SEE studies. Specifically, if no reliable theoretical or experimental data for δ_m and E_m exist, such data can be obtained from Monte Carlo simulations and be used to quantify the SEE yields for new materials by using the "universal law". Such extensive analysis has been done by Lin and Joy [8], who obtained the universal law parameters for 44 elements with Z = 3–83.

2.2. Monte Carlo codes

Several researchers have developed Monte Carlo codes based on the above theory that are applicable to low-energy SEE-yield calculations [3,4,7–9]. The Rutherford cross-section for elastic electron scattering of low-E electrons and high-Z materials was replaced by Mott's cross-section, which was tabulated for the electron energies in the range of 1–100 keV [3]. The inelastic energy loss of electrons is usually approximated by Bethe's equation:

$$\frac{dE}{dS} = -78,500 * \frac{Z}{AE} * \log_e\left(\frac{1.166E}{J}\right), \tag{10}$$

where dE/dS is the stopping power of the target, E is the energy of the primary electrons, Z is the atomic number, A is the atomic weight, and S is the product of the density ρ (g/cm^3) and the distance traveled by the electron. J is the mean ionization energy of the target material and is obtained from experiment. This variable includes all inelastic energy mechanisms and allows researchers to study the energy loss in a compact and simple way by using the Bethe equation. The experimental value of J for Al_2O_3 is 145 eV [7,9]. There are no measured values of J for ZnO and MgO.

Berger and Seltzer (see e.g. p. 32 in book [9]) proposed an empirical formula applicable to high-energy electrons as follows:

$$J = \left[9.76Z + \frac{58.5}{Z^{0.19}}\right] * 10^{-3} \quad (\mathrm{keV}). \tag{11}$$

For compound materials (e.g. ZnO), an averaged value for atomic number can be used:

$$Z_{av} = (1 * Z_{Zn} + 1 * Z_O)/2, \tag{12}$$

which gives J_{ZnO} = 219 eV and J_{MgO} = 135 eV.

The Bethe approximation (10) was improved by Seiler [12] for low-energy electrons.

Two important simulation parameters in the Monte Carlo model shown in Eq. (6). One is ε, the average energy for producing secondary electron, and the other is the escape depth λ. These two parameters have a significant impact on the simulation result. We used ε = 20 eV for Al_2O_3 [10].

The escape depth λ of insulators can be relatively large compared to that of metal surfaces, a direct effect of the small absorption coefficient of low-energy electrons in insulators because of the large energy band gap (e.g. E_g = 8 eV in Al_2O_3). Kanaya et al. [11] proposed a theoretical model for calculating the escape depth for a range of insulators and alkaline materials. Based on this analysis,

the escape length can be chosen as $\lambda = 60$ Å for Al_2O_3. This value was also suggested by Joy [10].

2.3. Angular dependence

SEE yield at high primary electron energies $E_{PE} > 1$ MeV increases as the angle of incidence θ relative to the normal increases ($\theta < 80°$), with the exception of grazing angles. This is caused by a decrease of λ:

$$\delta(\theta) = \delta_0(\cos\theta)^{-n}. \tag{13}$$

The power exponent $n = 1$ is applicable for the target materials with Z approximately equal to 30 [12]. This law is not applicable to the electrons with low and intermediate energies typical for MCP development.

Ohya and Mori [15] have studied the SEE yield at lower energies, ~100 eV. They found that Eq. (13) can fail at low energies.

3. Empirical models

Ito et al. [18] proposed the following empirical model for calculating the average number of emitted electrons:

$$\delta(\theta_i, \varepsilon_i) = 4\nu_i \cdot \delta_m(\theta_i)/\{\varepsilon_m(\theta_i) \cdot (1 + \varepsilon_i/\varepsilon_m(\theta_i))^2\}, \tag{14}$$

where θ_i and ε_i are incident angle and energy of the electron hitting the target's surface, respectively, and $\delta_m(\theta_i)$ and $\varepsilon_m(\theta_i)$ are the maximum yield and the incident energy for the maximum yield, respectively:

$$\begin{aligned} \delta_m(\theta_i) &= \delta_{m0} \cdot \exp[\alpha(1 - \cos\theta_i)], \\ \nu_m(\theta_i) &= \nu_{m0}/\sqrt{\cos\theta_i}. \end{aligned} \tag{15}$$

Here δ_{m0} is the maximum yield corresponding to the electrons with incident angle normal to the surface, ν_{m0} is the incident energy for the maximum yield, and α is the material constant.

Guest et al. [19] developed another empirical SEE-yield model that contains Eq. (15) as correct experimental input data. The reduced SEE yield is obtained by the following equation,

$$\delta/\delta_m(0) = \left(\frac{\varepsilon}{\varepsilon_m}\sqrt{\cos\theta}\right)^{\beta} \exp[\alpha(1 - \cos\theta)] + \beta\left(1 - \frac{\varepsilon}{\varepsilon_m}\sqrt{\cos\theta}\right), \tag{16}$$

where β is the adjustable parameter chosen to fit the experimental SE yields at normal electron incidence.

Fig. 1 shows a comparison of the above empirical models of the secondary electron emission yields at normal incidence in reduced form. The maximum yields and the incident energies at maximum for all models were chosen to be the same as for Ito's model: $\delta_m = 4$ and $\varepsilon_m = 250$ eV. Baroody [20] and Lye and Dekker [21] proposed a model that can be reduced to the following simple form:

$$\begin{aligned} \delta/\delta_m &= \frac{1}{F(0.92)} F(0.92E_0/E_{0m}), \\ F(r) &= \exp(-r^2)\int_0^r \exp(y^2)dy. \end{aligned} \tag{17}$$

Agarwal [22] proposed a new formula that improves the high-energy behavior of the Lye–Dekker and Ito's models and can be represented by the following formula:

$$\delta/\delta_m = \frac{2(E_0/E_{0m})}{1 + (E_0/E_{0m})^{1.85(2Z/A)}}, \tag{18}$$

where Z and A are the atomic number and atomic weight.

These four models are compared in Fig. 1. The maximum yields and the incident energies at maximum for all models are the same as for Ito's model: $\delta_m = 4$ and $\varepsilon_m = 250$ eV. This comparison shows that the empirical models give significant deviation at the energies higher than that of the maximum and therefore they cannot be used to predict the SEE data for various materials. Moreover, the angular dependences of the SEE in empirical models are drastically different and inconvenient for comparison.

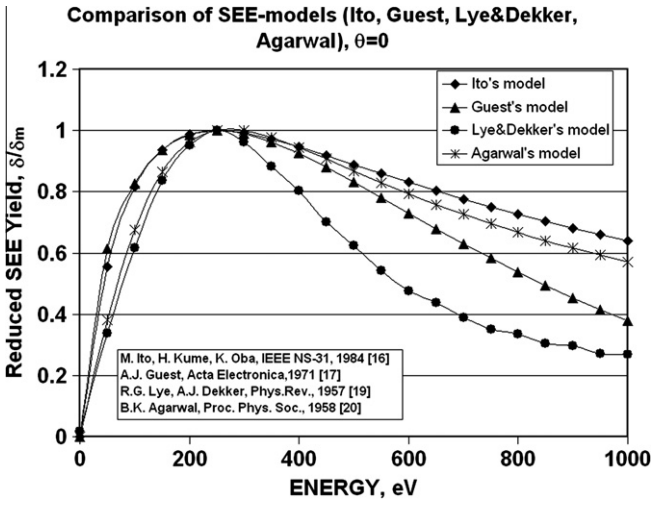

Fig. 1. Comparison of the empirical models of the secondary electron emission yields in reduced form at normal incidence. The maximum yields and the incident energies at maximum for all models were chosen to be the same as for Ito's model: $\delta_m = 1$ and $\varepsilon_m = 250$ eV.

4. Simulation results

The simulation results for the electron energies above ~200 eV were obtained by using Monte Carlo codes developed in [3,4,4–10]. A detailed explanation of the algorithm used in these codes can be found elsewhere (see, e.g. [3,7]). For electrons with energies below ~200 eV, Eq. (10) was modified according to the algorithm proposed by Joy [9]. Since Eq. (9) is not valid for electron energies below 50 eV, we used the "universal law of SEE yield" given by Eq. (9) for the low-energy region below 50 eV.

The main adjustable parameters of the Monte Carlo simulations are the escape length λ and the average energy per secondary electron emission ε that were used in Eq. (6) [7–11]. The escape length of ZnO was used as an adjustable parameter. The following material's parameters were used: λ was varied between 40 Å for low- and 20 Å for high-energy regions, according to a suggestion by Joy [9], and $\varepsilon = 125$ eV [11]. These parameters are listed in Table 1.

The results of our simulations are presented in Figs. 2–6. Fig. 2 shows a two-dimensional plot of the secondary emission yield generated by primary electrons with energies of $E = 50$–2000 eV and incident angles in the range of $0° \leqslant \theta_i \leqslant 89°$ bombarding a Al_2O_3 substrate. Figs. 3 and 4 show the energy and angular dependences of the SEE yield of electrons colliding with a Al_2O_3 surface at incident angles $0 \leqslant \theta_i \leqslant 89°$ and comparison of the calculated data with the results of experiments obtained by Dawson [23]. The parameterized data shown in Fig. 3 are then submitted as input

Table 1
Material parameters.

Material	ε, eV	λ, Å
Al_2O_3	20 [9]	60 [10]
MgO	20 [11]	120 [11]
ZnO	125 [11]	30 [this work]

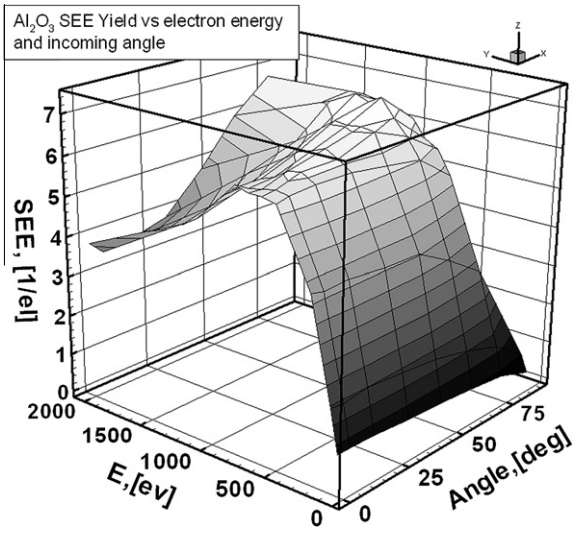

Fig. 2. SE yield generated by primary electrons with energies of $E = 50–2000$ eV and incident angles in the range of $0° \leqslant \theta_i \leqslant 89°$ obtained in this paper by MC simulation.

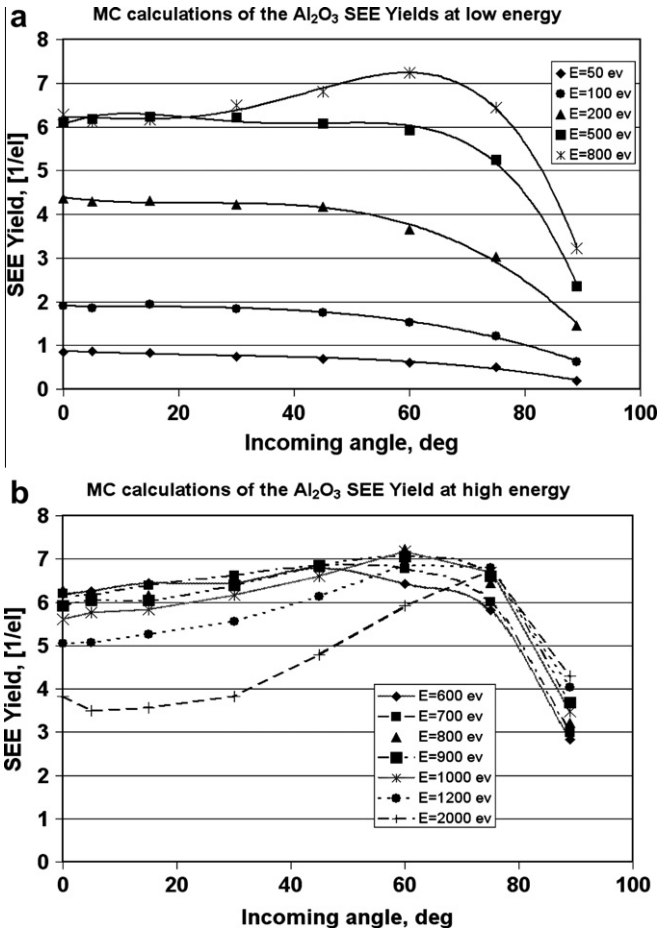

Fig. 3. SE yields generated by electrons colliding with a 5 nm Al_2O_3 thin film, with energies $E = 50–2000$ eV and incident angles in interval $0° \leqslant \theta_i \leqslant 89°$: (a) $E = 50–800$ eV and (b) $E = 600–2000$ eV.

data for a Monte Carlo trajectory code that models the entire micro-channel plate (MCP) device. The results of the whole MCP device simulations will be published separately elsewhere.

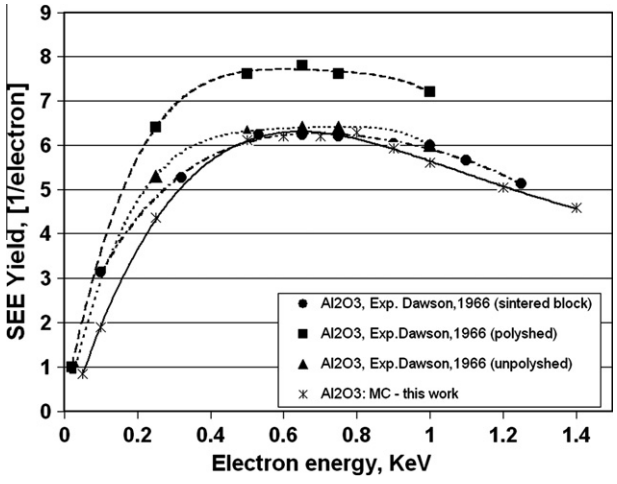

Fig. 4. Comparison of our results calculated at normal electron incidence by Monte Carlo method for Al_2O_3 with experimental data obtained by Dawson [23] for polished (squares and dashed line), unpolished (triangles and dotted line), and sintered surface (circles and dash-dotted) curves and symbols. Our simulation is shown as stars symbols and fitted by solid curve.

5. Comparison with experiment

Since the charging of highly resistive ceramics gives incorrect SEE-yield results, it is important to compare the experimental measurements with the Al_2O_3 emission rates obtained by Monte Carlo simulations. Dawson measured SEE yields of an Al_2O_3 surface by using a pulsed technique that guaranteed that if the surface was charged, it could be replenished by a very low-energy electron shower between the two pulses [23].

Fig. 4 shows that experimental results are different for different type of sample used in experiment. The highest SEE yield was observed for a smooth, polished surface, whereas unpolished and sintered samples showed 18% lower SEE yield at the maximum. The difference is much smaller at the lower energies that are more important for the operation of the MCP device since the average electron energy is about 100 eV [19].

Fig. 4 shows close agreement between experiment and simulation, which is important because mathematical difficulties have resulted in almost no theory for low-energy electron emissions.

Our Monte Carlo simulation did not use any additional experimental data; the important parameters were obtained from empirical theories. However, since these theories are often not applicable to low-energy electrons typical of MCP operation, we can assume that the escape length for the electrons in Al_2O_3 is an adjustable parameter, rather than calculated from theory. Other parameters of Al_2O_3 that were used to generate the SEE yield shown in Figs. 2–4 are as follows: $Z_{av} = 10$; $A_{av} = 20.39$, where "av" means averaging for compound material; and $\rho = 3.9$ g/cm^3.

Our MC simulations were also conducted for the SEE yields of ZnO samples, and the results of our simulations were compared with the experimental results by Gornyi [26]. This author studied SEE of a single crystal of Zn with two faces (0 0 0 1 and $1\,0\,\bar{1}\,0$) and a polycrystalline Zn covered with a thin hexagonal ZnO single crystal films (with the thickness of 20–30 Å), where the structure of these films matched that of the Zn substrate structure.

Fig. 5 shows a comparison of our Monte Carlo simulations (stars and solid line) with the measurements of SEE from a $(1\,0\,\bar{1}\,0)$ face of Zn covered with a thin ZnO single crystal film. The agreement between the simulated and measured data is close at the maximum of SEE yield but less comparable at the low-energy end. This discrepancy can be explained by the fact that the thickness of the film was too small and the electrons were able to penetrate into the substrate below the film.

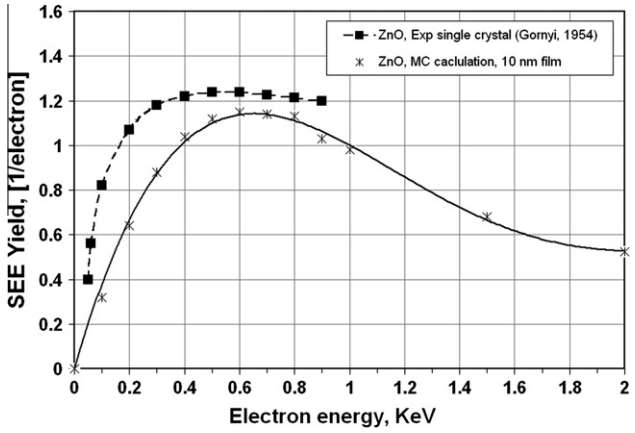

Fig. 5. Comparison of the Monte Carlo simulation results at normal electron incidence angle for ZnO with experimental data obtained by Gornyi [26] for a Zn single crystal covered with a crystalline metal films of ZnO (diamonds and dashed line). Our simulation is shown as circles and solid curve that was fitted to the calculated data points.

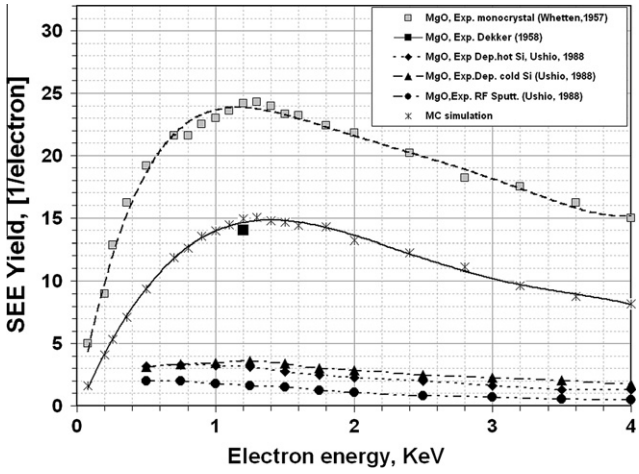

Fig. 6. Comparison of the Monte Carlo simulation results for MgO with experimental data obtained by Whetten and Laponsky [27] for a MgO single crystal and three data sets obtained by Ushio et al. [28] for thin MgO films deposited on various substrates, (diamonds and dashed line). Our simulation is shown as circles and solid curve that was fitted to the calculated data points.

Our MC results also were compared with MgO data measured by Whetten and Laponsky [27] and Ushio et al. [28]. There is a big difference between the results measured for single crystalline [25] and thin MgO films obtained via the electron beam evaporation technique and deposited on different silicon substrates and those for a MgO film deposited via rf magnetron sputtering. The films were 100 nm in thickness on a Si(1 1 1) surface and stainless steel substrates.

Since the experimental SEE yields from different MgO surfaces differ significantly, our simulations should be coupled with the data obtained in experiment for the escape length λ and the average energy per secondary electron emission ε that were used in Eq. (6) [9].

Our MgO simulations were implemented for the following parameters: $\lambda = 120$Å and $\varepsilon = 20$ eV [7].

We have obtained good comparison with one data point measured by Dekker [29].

6. Summary and future work

MCP gain and transient time simulations are closely related to the SEE yields calculated in this paper. The theory of SEE yields at low electron energies is limited. Therefore, the simulations and comparison to experiment for such yields are important. The SEE yields are expressed as a parameterized function of two variables: primary electron energy and incident angle. In this paper, we have presented an approach that combines Monte Carlo simulation of the secondary electron emission with empirical SEE theories and experiment. We showed that this approach gives a close agreement for Al_2O_3, for which extensive experimental data and theory exist for obtaining important simulation parameters such as energy and escape length of secondary electrons. This parameterization work is ongoing, and the results will be published elsewhere.

The main problem in calculating the SEE coefficients for all materials is the lack of understanding of electron emission in the low-energy region where theory and simulation models are insufficient. Fortunately, the empirical models give close results at electron energies below 100 eV. Therefore, one way of treating the SEE coefficients is combination of Monte Carlo calculation results at energies above ~200 eV with the data obtained via empirical models below this threshold.

We plan to calculate the SEE yields for those candidate materials having high emissive properties, such as Al_2O_3, a ZnO, mixture of Al_2O_3 + ZnO, and MgO. We will also simulate multilayer structures and vary the film thickness, in order to increase the yield.

In addition, we will calculate SEE yields of rough surfaces [24] and compare our results with a probability method developed by Furman and Pivi [25].

Acknowledgments

We thank D. Joy and P. Hovington for sharing their codes and giving valuable suggestions for the simulation parameters.

This work was supported by the US Department of Energy, under Contract DE-AC02-06CH11357.

References

[1] E. Nappi, Advances in the photodetection technologies for Cherenkov imaging applications, Nucl. Instr. Methods A 604 (2009) 190–192.
[2] S.M. Bradbury, R. Mirzoyan, J. Gebauer, E. Feigl, E. Lorenz, Test of the new hybrid INTEVAC intensified photocell for the use in air Cherenkov telescopes, Nucl. Instr. Methods A 387 (1997) 45–49.
[3] L. Reimer, D. Stelter, FORTRAN 77 Monte-Carlo program for minicomputers using Mott cross-section, Scanning 8 (1986) 265–277.
[4] S. Ishimura, M. Aramata, R. Shimizu, Monte-Carlo calculation approach to quantitative Auger electron spectroscopy, J. Appl. Phys. 51 (1980) 2853–2860.
[5] D.R. Beaulieu, D. Gorelikov, P. de Rouffignac, K. Saadatmand, K. Stenton, N. Sullivan, A.S. Tremsin, Novel microchannel plate device fabricated with atomic layer deposition, in: AVS Topical Conference on Atomic Layer Deposition, ALD 2009, Monterey, CA, July 19–22, 2009.
[6] J.A. Anderson1, K. Byrum1, G. Drake1, C. Ertley, H. Frisch, J.-F. Genat, E. May, D. Salek, F. Tang, New developments in fast-sampling analog readout of MCP based large-area picosecond time-of-flight detectors, IEEE-MIC 2008, ID-2973.
[7] D.C. Joy, Monte Carlo Modeling for Electron Microscopy and Microanalysis, Oxford University Press, 1995.
[8] Y. Lin, D.C. Joy, A new examination of secondary electron yield data, Surf. Interface Anal. 37 (2005) 895–900.
[9] D.C. Joy, A model for calculating secondary and backscattering electron yields, J. Microscopy 147 (1987) 51–64.
[10] D.C. Joy, Private Communication, 2009.
[11] K. Kanaya, S. Ono, F. Ishigaki, Secondary electron emission from insulators, J. Phys. D 11 (1978) 2425–2437.
[12] H. Seiler, Secondary electron emission in the scanning electron microscope, J. Appl. Phys. 54 (1983) R1–R18.
[13] J.R. Young, Penetration of electrons in Al_2O_3-films, Phys. Rev. 103 (1956) 292–293.
[14] R.O. Lane, D.I. Zaffarano, Transmission of 0–40 keV electrons by thin films with application to beta-ray spectroscopy, Phys. Rev. 94 (1954) 960–964.
[15] K. Ohya, I. Mori, Influence of backscattered particles on angular dependence of secondary electron emission from Copper, J. Phys. Soc. Jpn. 59 (1990) 1506–1517.
[16] V. Baglin, J. Bojko, O. Gröbner, B. Henrist, N. Hilleret, C. Scheuerlein, M. Taborelli, The secondary electron yield of technical materials and its variation with surface treatments, in: Proceedings of the EPAC, Vienna, Austria, 2000, pp. 217–221.

[17] K. Jakubka, B. Jüttner, On the influence of surface conditions on initiation and spot types of unipolar arcs in a Tokamak, J. Nucl. Mater. 102 (1981) 259–266.
[18] M. Ito, H. Kume, K. Oba, Computer analysis of the timing properties in micro channel plate photomultiplier tubes, IEEE Trans. NS-31 (1984) 408–412.
[19] A.J. Guest, A computer model of channel multiplier plate performance, Acta Electron. 14 (1971) 79–97.
[20] M. Baroody, A theory of secondary emission from metals, Phys. Rev. 78 (1950) 780–787.
[21] R.G. Lye, A.J. Dekker, Theory of secondary emission, Phys. Rev. 107 (1957) 977–981.
[22] B.K. Agarwal, Variation of secondary emission with primary electron energy, Proc. Phys. Soc. 71 (1958) 851–852.
[23] P.H. Dawson, Secondary electron emission yields of some ceramics, J. Appl. Phys. 37 (1966) 3644–3665.
[24] J. Kawata, K. Ohya, K. Nishimura, Simulation of secondary electron emission from rough surfaces, J. Nucl. Mater. 220–222 (1995) 997–1000.
[25] M.A. Furman, M.T.F. Pivi, Probabilistic model for the simulation of secondary electron emission, Phys. Rev. ST AB 5 (2002) 124404.
[26] N.B. Gornyi, Secondary electron emission for different faces of a Zn single crystal covered with crystalline zinc oxide films, JETP 26 (1954) 88–97 (in Russian).
[27] N.R. Whetten, A.B. Laponsky, Secondary electron emission of single crystals of MgO, J. Appl. Phys. 28 (1957) 515–516.
[28] Y. Ushio, T. Banno, N. Matuda, Y. Saito, S. Baba, A. Kinbara, Secondary electron emission studies on MgO films, Thin Solid Films 167 (1988) 299–308.
[29] A.J. Dekker, Secondary electron emission, in: F. Seitz, D. Turnbull, H. Ehrenreich (Eds.), Solid State Physics, vol. 6, Academic Press, NY, 1958, pp. 251–311.